Title
A STUDY OF THE REACTIONS K""p * u* rt* (?|) BETWEEN .85 AND 1.15 GeV/c

Author
Kane, Daniel F.

Publication Date
1971-04-01

D. Kane, Jr.

UCRL-20676
UC-34 Physics
TID-4500 (57th Ed.)

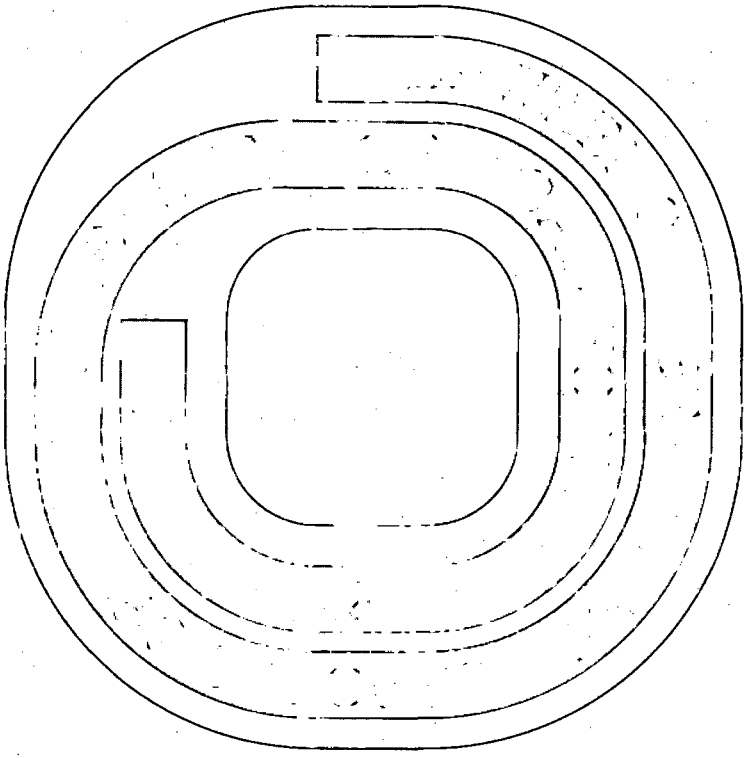

A STUDY OF THE REACTIONS $K^- p \to \Sigma^{\pm} \pi^{\mp} (\pi^0)$ BETWEEN .85 AND 1.15 GeV/c

Daniel F. Kane, Jr.

April 1971

AEC Contract No. W-7405-eng-48

DISCLAIMER

UCRL-20676

A Study of the Reactions $K^-p \to \Sigma^{\pm}\pi^{\mp}(\pi^o)$ Between .85 and 1.15 GeV/c

Daniel F. Kane, Jr.

April 1971

Abstract

We present data for the reactions $K^-p \to \Sigma^{\pm}\pi^{\mp}(\pi^o)$ for laboratory momenta between .85 and 1.15 GeV/c: angular distributions, polarizations and Legendre coefficients for $\Sigma^{\pm}\pi^{\mp}$; Dalitz plots and invariant mass-squared plots for $\Sigma^{\pm}\pi^{\mp}\pi^o$; and cross sections for all reactions. For the two body final states we also present results of a partial wave analysis based primarily on this data. In particular we present the resonance parameters for the D15, D05, and F05 waves found in this analysis.

We would like to emphasize at this point that this is only a companion report to Ref. 4. We have used most of the techniques of data handling and analysis described in that report and no details are reproduced here. Since the data described in this report and that in Ref. 4 came from different exposures, and since some techniques were different, we present this data separately.

I. Introduction

A preliminary report of this data has been reported elsewhere, including a partial wave analysis of the incomplete data.[1] The cross sections reported at that time were in serious disagreement with values presented elsewhere.[2] We have now renormalized the beam path length and weighted the events using a different procedure; the results are in better agreement with Ref. 2.[3] Besides renormalizing and reweighting, we have redone the kinematic fitting using a two vertex fit. This did not result in significant change for the two body final states; however, by this procedure we obtained the results for the three body final states. An ionization scan was performed to resolve ambiguities--either between the two decay modes of the Σ^+ or between equally good (kinematically) but distinct solutions for the three body final states. The kinematic fitting procedure, the ionization scan, and the weighting procedure have been described elsewhere for another experiment.[4] We only note that the results presented in Ref. 1 were based on a weighting procedure in which an average weight was estimated for each bin in the angular distribution; following Ref. 4 we have weighted events individually. In this report we wish to describe the techniques used to renormalize the path length and the method of estimating the scanning and throughput efficiencies. We then present the experimental results as well as resonance parameters from a partial wave analysis based primarily on this data.

II. Procedures

We have based our path length normalization on a high statistics beam count performed for the study of another reaction using this

film.[5] It was not possible just to use the path lengths obtained in that study since our study used a slightly different subset of the film. The events studied in Ref. 5 were measured on the Flying Spot Digitizer, and some rolls could not be measured on the FSD because of either light tracks or excessive overlap of tracks. The events for our experiment were measured manually on Franckensteins and most of the rolls could be used; however, in the several years between the measurements and our refitting of these measurements some data were lost through misplaced tapes or erasures. We determined the path length for the rolls used in both studies, scaling the path lengths given in Ref. 5 by the ratio of the total number of good events in common rolls to the total number of good events in all rolls used by Ref. 5. For this we counted good events of both fitted event types:

$$K^- p \to \bar{K}^0 n$$

$$K^- p \to \pi^0 \Lambda$$

From this we could determine the path length in the rolls used for our experiment, scaling the path length of the common rolls by the appropriate ratio of numbers of good events. For this we counted good events in all four reactions; thus the statistical uncertainty in the final path lengths did not contribute seriously to the uncertainties in the cross sections for individual reactions. The resulting path lengths are listed in Table I; the distribution of fitted beam momenta is shown in Fig. 1.

The fiducial volume cuts were necessarily the same as those in Ref. 5; we include them in Table I for completeness. The distributions in the top non-Gaussian parameters, as well as the cuts made in these

parameters, are shown in Fig. 2. The distribution of events with respect to the accepted region for the decay vertex is shown in Fig. 3. See Ref. 4 for definition of all quantities. In Table II we list the other cuts applied to the length of the Σ track and the decay angles. These cuts are quite similar to those made in Ref. 4, the main difference being a much shorter L_{MAX}. The earlier scanners seemed to disassociate decays of very long tracks. The results of the cuts are given in Table III. The differential lifetime distributions for each reaction and decay mode are shown in Fig. 4; and the mean lifetimes for events passing all cuts are given in Table IV. The latter were obtained by maximum likelihood technique.[6] The values for the $\Sigma^+ \to \pi^0 p$ decay mode are in significant disagreement with accepted values.[7] Since this result is probably due to missing events for short tracks and some (relatively few) fake events at large lifetimes, we are not too concerned about contamination (we used these events only to determine polarizations, so missing events was not serious). The distributions in the decay angles, which should be isotropic (see Ref. 4), are shown in Fig. 5.

In order to determine the scanning efficiency we had about 10% of the rolls rescanned by the personnel who scanned for the experiment reported in Ref. 4. The original scan and the rescan had comparable efficiencies for all events; however, since the film was generally of somewhat poorer quality than that of the more recent experiment, we assigned a somewhat lower scanning efficiency for events passing all cuts than those given in Ref. 4. Since this was not an accurate determination we assigned a fairly large error; we used the same value for all momenta

scanning efficiency - .92 ± .06

The values of the throughput efficiencies--fraction of the true events (seen) which get through to the analysis stage--were likewise rough estimates. This efficiency takes into account both bookkeeping losses and loss of true but poorly measured events which were not properly fitted. The former could be determined from records; the latter were estimated from the fits with poor χ^2, as was done in Ref. 4. The throughput efficiencies are listed in Table IV.

III. Results

All procedures used for processing the data to obtain cross sections, angular distributions, polarizations, Legendre coefficients, Dalitz plots and invariant mass-squared distributions have been thoroughly discussed in Ref. 4. We shall only present the results for this set of data; all figures and tables that we shall refer to in this section have analogues in that report. For these results we have grouped some of the momenta together, as is indicated in Table V. This table gives the cross sections. In Table VI we present the raw data for the two body final states. The grouping of bins and the values and errors are indicated in Fig. 6 for the angular distributions and in Fig. 7 for the polarizations. The Legendre coefficients are given in Table VII and the resulting function dependence of the polarizations is shown in Fig. 7, of the angular distributions in Fig. 8. The Dalitz plots and invariant mass-squared distributions are shown in Fig. 9.

IV. Resonance Parameters

We have performed a partial wave analysis of the two body final states for this data plus the data at the lowest energy of Ref. 4. We have used the methods of Ref. 4 except that resonances were allowed to have arbitrary phase. We fit the Legendre coefficients and then, starting from that solution, fit directly to the cross sections, angular distributions, and polarizations. We obtained four good fits, which are shown in Table VIII for the direct fit to the data. The waves S01 to D13 as well as F15 and F17 had P(4) parameterizations (nomenclature of Ref. 4), the parameterizations of D05, D15, and F05 are shown. As we have pointed out earlier, some waves have rapid clockwise movements, which violate the Wigner condition for causality.[8] The last two columns of Table VIII indicate the worst wave and its angular speed (in radians per pion mass).

Initially, we started from the best solution of Ref. 1. This solution did not include the $\Sigma(1765)$ resonance in D15; the $\Lambda(1830)$ in D05 was accompanied by a background term. Almost immediately we found that both resonances were present with very little background. We tried starting all non-resonant waves from zero, as is described in Ref. 4, varying the structure in the D5 waves. Some background is needed, probably in the D15 which resonates low in the energy range. The resonance parameters we obtained in these fits are given in Table IX; again the nomenclature is that of Ref. 4.

References

1. R. Bell, Phys. Rev. Letters 19, 936 (1967).
2. R. Armenteros, et al., Nuclear Physics B8, 233 (1968).
3. There are still significant, though not serious, discrepancies in the $\Sigma^- \pi$ final state; more data at these energies would be useful. We understand that such an experiment is underway (I. Butterworth, Rutherford, private communication, April 1971).
4. Daniel Frederick Kane, Jr., UCRL-20682 (Ph.D. Thesis), April 1971 (unpublished).
5. James Louie, UCRL 18411 (Ph.D. Thesis), August 1968 (unpublished).
6. a. M. S. Bartlett, Phil. Mag. 44, 249 (1953).
   b. J. Louie, Powell-Birge (LRL) Physics Note 104, December 1966.
7. Particle Data Group, Physics Letters 33, B1 (1970).
8. D. Kane et al., UCRL-19790, August 1970 (unpublished).

Table I. Beam Normalization

Momentum	BETE Cut*	Path Length (KM)	Microbarn Equivalents
.867 ± .010	360.3 ± 2.6	73.7 ± 5.2	3.70 ± .26
.882 ± .008	359.9 ± 2.6	29.5 ± 1.5	9.25 ± .46
.916 ± .011	358.3 ± 3.0	324.5 ± 21.3	.84 ± .055
.936 ± .011	359.0 ± 2.4	24.8 ± 1.4	11.00 ± .60
.975 ± .026	357.7 ± 2.7	336.5 ± 19.5	.81 ± .047
1.010 ± .013	357.4 ± 2.5	420.0 ± 22.6	.65 ± .035
1.053 ± .013	357.1 ± 2.4	229.0 ± 11.5	1.19 ± .06
1.109 ± .014	356.5 ± 2.6	88.5 ± 6.3	3.08 ± .22

XVTX Cut	29.0 → 62.0
YEND Cut	34.0 → 64.0
ALFE Cut*	90.0 ± 2.4

*For distributions the acceptance was 1.5 times greater.

Table II. Cuts Used

	L_{MIN} (cm)	L_{MAX} (cm)	τ_k (nsec.)	θ (deg.)	ϕ (deg.)
Cross sections					
$K^- \to \pi^- n$	.5	7.5	.5	5.0	30.
$\Sigma^+ \to \pi^o p$	.6	7.5	.3	7.5	50.
$\Sigma^+ \to \pi^+ n$	.5	7.5	.3	5.0	30.
Distributions					
$\Sigma^- \to \pi^- n$	.3	7.5	.5	5.0	0.
$\Sigma^+ \to \pi^o p$	.3	7.5	.3	5.0	0.
$\Sigma^+ \to \pi^+ n$	.3	7.5	.3	5.0	0.

Table III. Effects of Cuts

	Fail Phase Space or Chamber Volume Cuts	Fail Length or Angle Cuts	Pass All Cuts
Cross sections			
$\Sigma^- \to \pi^- n$	2124	2258	3984
$\Sigma^+ \to \pi^o p$	868	1664	1186
$\Sigma^+ \to \pi^+ n$	1251	1486	2237
Distributions			
$\Sigma^- \to \pi^- n$	1964	462	5940
$\Sigma^+ \to \pi^o p$	811	252	2655
$\Sigma^+ \to \pi^+ n$	1164	332	3478

Table IV.

Mean Lifetimes

Mean Life (nsec.)	$K^- p \to \pi \Sigma$	$K^- p \to \pi \Sigma \pi^0$
$\Sigma^- \to \pi^- n$	.151 ± .005	.163 ± .006
$\Sigma^+ \to \pi^0 p$	.090 ± .003	$.100 \begin{smallmatrix} + .007 \\ - .005 \end{smallmatrix}$
$\Sigma^+ \to \pi^+ n$	.086 ± .003	.088 ± .004

Throughput Efficiencies

Momentum	Efficiency
.867	.90 ± .04
.882	.86 ± .04
.916	.92 ± .04
.936	.86 ± .04
.975	.80 ± .04
1.010	.89 ± .04
1.053	.88 ± .04
1.109	.88 ± .04

Table V. Cross Sections

A. $K^- p \to \pi^+ \Sigma^-$

P_{LAB} GEV/C	UNWEIGHTED NUMBER	AVERAGE WEIGHT	E_{CM} GEV	$\sigma \pm \Delta\sigma$ (mb)
.867	136	2.14	1.732	1.169 ± .143
.882	33	2.16		
.916	508	2.10	1.754	1.066 ± .115
.936	39	2.12		
.975	431	2.13	1.782	1.009 ± .113
1.010	678	2.15	1.798	1.151 ± .119
1.053	400	2.19	1.818	1.287 ± .137
1.109	174	2.18	1.844	1.441 ± .189

B. $K^- p \to \pi^- \Sigma^+$

P_{LAB} GEV/C	UNWEIGHTED NUMBER	AVERAGE WEIGHT	E_{CM} GEV	$\sigma \pm \Delta\sigma$ (mb)
.867	74	2.39	1.732	1.658 ± .228
.882	27	2.43		
.916	360	2.41	1.754	1.761 ± .197
.936	14	2.20		
.975	268	2.38	1.782	1.480 ± .174
1.010	457	2.35	1.798	1.797 ± .192
1.053	220	2.43	1.818	1.669 ± .193
1.109	74	2.51	1.844	1.495 ± .236

XBL 714-757

Table V. Cross Sections (Cont.)

C. $K^- p \to \pi^+ \Sigma^- \pi^0$

P_{LAB} GEV/C	UNWEIGHTED NUMBER	AVERAGE WEIGHT	E_{CM} GEV	$\sigma \pm \Delta\sigma$ (mb)
.867	76	2.04	1.732	.627 ± .088
.882	19	2.05		
.916	392	2.03	1.754	.789 ± .087
.936	26	2.10		
.975	306	2.04	1.782	.685 ± .079
1.010	414	2.04	1.798	.668 ± .072
1.053	231	2.06	1.818	.698 ± .080
1.109	121	2.05	1.844	.946 ± .133

D. $K^- p \to \pi^- \Sigma^+ \pi^0$

P_{LAB} GEV/C	UNWEIGHTED NUMBER	AVERAGE WEIGHT	E_{CM} GEV	$\sigma \pm \Delta\sigma$ (mb)
.867	41	2.21	1.732	.835 ± .140
.882	15	2.27		
.916	182	2.32	1.754	.907 ± .111
.936	17	2.31		
.975	116	2.27	1.782	.612 ± .084
1.010	202	2.32	1.798	.783 ± .093
1.053	122	2.29	1.818	.871 ± .114
1.109	48	2.27	1.844	.879 ± .157

XBL 714-756

Table VI. Raw Data in Twenty Equal Bins of the Production Cosine, cos θ.

A. $K^- p \to \pi^+ \Sigma^-$

NUMBER WEIGHTED / NUMBER UNWEIGHTED

CENTER	1.732 GEV	1.754 GEV	1.782 GEV	1.798 GEV	1.818 GEV	1.844 GEV
-.95	19.7/ 15	95.1/ 71	44.7/ 33	63.1/ 46	45.9/ 33	18.4/ 13
-.85	33.9/ 26	100.6/ 76	103.3/ 77	152.3/112	93.6/ 68	33.6/ 24
-.75	36.2/ 28	123.0/ 94	118.4/ 89	165.5/123	89.8/ 66	29.1/ 21
-.65	32.1/ 25	106.3/ 82	85.5/ 65	111.6/ 84	72.9/ 54	31.4/ 23
-.55	10.2/ 8	79.7/ 62	66.5/ 51	105.3/ 80	50.5/ 38	18.9/ 14
-.45	23.9/ 19	62.4/ 49	37.3/ 29	70.2/ 54	27.6/ 21	17.3/ 13
-.35	12.6/ 10	37.8/ 30	38.3/ 30	42.4/ 33	19.5/ 15	5.3/ 4
-.25	6.2/ 5	35.0/ 28	30.3/ 24	16.6/ 13	7.7/ 6	3.9/ 3
-.15	1.2/ 1	26.0/ 21	13.8/ 11	29.0/ 23	14.0/ 11	6.4/ 5
-.05	2.4/ 2	22.1/ 18	26.0/ 21	24.9/ 20	17.5/ 14	5.1/ 4
+.05	8.5/ 7	26.8/ 22	31.9/ 26	38.3/ 31	21.1/ 17	7.5/ 6
+.15	6.1/ 5	31.5/ 26	23.2/ 19	51.4/ 42	17.2/ 14	13.6/ 11
+.25	14.5/ 12	34.9/ 29	21.8/ 18	64.3/ 53	35.3/ 29	24.5/ 20
+.35	8.4/ 7	46.8/ 39	24.1/ 20	37.3/ 31	26.6/ 22	20.6/ 17
+.45	15.7/ 13	34.8/ 29	21.6/ 18	37.3/ 31	31.2/ 26	15.6/ 13
+.55	15.9/ 13	25.5/ 21	13.3/ 11	22.9/ 19	26.4/ 22	13.2/ 11
+.65	12.5/ 10	22.3/ 18	11.1/ 9	13.5/ 11	11.0/ 9	10.9/ 9
+.75	12.9/ 10	35.7/ 28	11.4/ 9	22.7/ 18	18.8/ 15	9.9/ 8
+.85	31.2/ 23	43.9/ 33	33.5/ 25	82.1/ 62	39.3/ 30	28.6/ 22
+.95	24.8/ 16	70.2/ 46	68.4/ 46	131.7/ 89	110.5/ 75	47.5/ 33
TOTAL	328.8/255	1060.4/822	824.5/631	1282.2/975	776.4/595	361.1/274

B. $K^- p \to \pi^- \Sigma^+$

(Data From $\Sigma^+ \to \pi^+ n$ Only)

NUMBER WEIGHTED / NUMBER UNWEIGHTED

CENTER	1.732 GEV	1.754 GEV	1.782 GEV	1.798 GEV	1.818 GEV	1.844 GEV
-.95	12.1/ 10	42.3/ 35	35.1/ 29	43.7/ 36	29.2/ 24	4.9/ 4
-.85	12.1/ 10	26.5/ 22	27.8/ 23	44.8/ 37	29.1/ 24	18.3/ 15
-.75	15.7/ 13	39.8/ 33	27.8/ 23	47.2/ 39	31.5/ 26	4.9/ 4
-.65	6.0/ 5	25.3/ 21	26.5/ 22	37.4/ 31	15.7/ 13	8.5/ 7
-.55	8.5/ 7	15.7/ 13	13.3/ 11	19.3/ 16	14.5/ 12	2.4/ 2
-.45	4.9/ 4	23.0/ 19	3.6/ 3	6.0/ 5	6.0/ 5	0. / 0
-.35	3.7/ 3	13.4/ 11	6.0/ 5	7.2/ 6	0. / 0	0. / 0
-.25	2.5/ 2	6.1/ 5	7.3/ 6	3.6/ 3	1.2/ 1	1.2/ 1
-.15	2.5/ 2	17.2/ 14	2.4/ 2	4.9/ 4	0. / 0	0. / 0
-.05	10.0/ 8	19.8/ 16	4.9/ 4	17.2/ 14	7.3/ 6	8.5/ 7
+.05	5.1/ 4	17.5/ 14	14.9/ 12	28.4/ 23	3.7/ 3	0. / 0
+.15	12.8/ 10	29.1/ 23	22.6/ 18	42.4/ 34	19.9/ 16	13.6/ 11
+.25	14.3/ 11	34.7/ 27	35.5/ 28	54.4/ 43	20.1/ 16	5.0/ 4
+.35	14.5/ 11	54.9/ 42	54.2/ 42	66.8/ 52	37.0/ 29	8.9/ 7
+.45	22.9/ 17	79.8/ 60	46.2/ 35	96.7/ 74	20.7/ 16	6.5/ 5
+.55	23.6/ 17	80.5/ 59	72.9/ 54	69.7/ 52	34.6/ 26	7.9/ 6
+.65	17.3/ 12	99.3/ 70	68.6/ 49	98.2/ 71	24.7/ 18	20.4/ 15
+.75	25.9/ 17	62.8/ 42	50.0/ 34	82.9/ 57	36.2/ 25	22.8/ 16
+.85	21.8/ 13	70.0/ 43	44.5/ 28	98.2/ 62	43.9/ 28	24.9/ 16
+.95	7.9/ 4	47.9/ 24	23.2/ 11	53.2/ 27	56.6/ 29	42.8/ 22
TOTAL	243.6/180	805.7/593	587.4/439	922.2/686	432.0/317	201.4/142

XBL 714-760

Table VI. Raw Data in Twenty Equal Bins of the Production Cosine, cos θ (cont.)

C. $K^- p \to \pi^- \Sigma^+$

(Data From $\Sigma^+ \to \pi^0 p$ Only)

SUM OF POLAR COSINE / NUMBER UNWEIGHTED

CENTER	1.732 GEV	1.754 GEV	1.782 GEV	1.798 GEV	1.818 GEV	1.844 GEV
-.95	1.5/ 6	-3.3/ 15	-1.8/ 8	-3.0/ 11	-1.8/ 9	.6/ 7
-.85	-1.5/ 11	-2.2/ 17	-4.8/ 14	-7.9/ 29	-8.2/ 13	2.4/ 8
-.75	.0/ 9	-.2/ 16	-4.2/ 15	-5.5/ 18	-1.9/ 8	1.7/ 5
-.65	-1.1/ 5	-2.5/ 19	-4.2/ 10	-3.2/ 18	-1.9/ 6	1.2/ 4
-.55	1.2/ 4	-4.6/ 16	-3.5/ 10	-2.4/ 6	-1.5/ 2	1.6/ 3
-.45	.3/ 4	.9/ 4	-2.4/ 5	-.6/ 5	1.3/ 2	-.8/ 1
-.35	-.9/ 7	-1.6/ 5	-.8/ 7	-1.0/ 4	-.3/ 1	0. / 0
-.25	1.0/ 1	-2.5/ 3	.7/ 1	.4/ 1	0. / 0	0. / 0
-.15	-.1/ 5	.2/ 6	1.9/ 4	.2/ 3	0. / 0	-.7/ 1
-.05	-.3/ 2	-1.1/ 5	1.4/ 4	2.3/ 7	-1.0/ 1	-.3/ 4
+.05	.6/ 4	1.9/ 6	7.6/ 13	5.1/ 11	1.4/ 3	-.1/ 2
+.15	1.7/ 4	6.4/ 16	3.2/ 6	1.4/ 18	-2.2/ 5	-2.0/ 7
+.25	1.8/ 5	5.3/ 22	8.6/ 29	5.1/ 24	.1/ 12	-1.1/ 3
+.35	3.4/ 11	11.1/ 32	7.3/ 29	3.8/ 37	5.6/ 15	.2/ 5
+.45	3.2/ 15	9.7/ 45	4.5/ 37	3.6/ 41	1.6/ 21	-.2/ 6
+.55	2.6/ 19	22.0/ 56	7.8/ 36	14.4/ 59	.9/ 32	-.2/ 4
+.65	5.0/ 17	8.5/ 48	19.5/ 42	10.4/ 55	8.7/ 25	4.0/ 10
+.75	5.8/ 16	15.6/ 59	10.9/ 37	26.5/ 64	12.9/ 31	.9/ 8
+.85	5.1/ 11	9.9/ 37	6.7/ 26	12.0/ 40	10.4/ 30	2.0/ 11
+.95	2.3/ 7	4.5/ 18	1.1/ 12	6.9/ 30	8.2/ 20	1.0/ 18
TOTAL	0. /163	0. /445	0. /345	0. /481	0. /236	0. /107

XBL 714-761

Table VII. Legendre Coefficients

A. From $K^- p \to \pi^+ \Sigma^-$ Angular Distributions

E_{CM}	$A_0 \times 10^{+3}$	$A_1 \times 10^{+3}$	$A_2 \times 10^{+3}$	$A_3 \times 10^{+3}$	$A_4 \times 10^{+3}$	$A_5 \times 10^{+3}$	$A_6 \times 10^{+3}$	$A_7 \times 10^{+3}$
1.732	73 ± 5	40 ± 10	31 ± 13	-62 ± 17	-47 ± 23	9 ± 32	-22 ± 33	-8 ± 33
1.754	84 ± 3	62 ± 6	44 ± 8	-66 ± 10	-57 ± 12	-5 ± 13	15 ± 14	13 ± 15
1.782	78 ± 3	50 ± 7	41 ± 8	-90 ± 10	-71 ± 12	8 ± 14	17 ± 14	-0 ± 18
1.798	100 ± 3	73 ± 7	62 ± 9	-85 ± 10	-68 ± 12	19 ± 15	-23 ± 15	-24 ± 18
1.818	97 ± 5	58 ± 12	124 ± 15	-24 ± 18	-4 ± 21	74 ± 25	16 ± 23	-28 ± 33
1.844	95 ± 8	104 ± 20	147 ± 27	40 ± 31	59 ± 37	52 ± 56	-95 ± 77	56 ± 10

B. From $K^- p \to \pi^- \Sigma^+$ Angular Distributions

E_{CM}	$A_0 \times 10^{+3}$	$A_1 \times 10^{+3}$	$A_2 \times 10^{+3}$	$A_3 \times 10^{+3}$	$A_4 \times 10^{+3}$	$A_5 \times 10^{+3}$	$A_6 \times 10^{+3}$	$A_7 \times 10^{+3}$
1.732	52 ± 3	-14 ± 6	52 ± 8	9 ± 9	-31 ± 11	48 ± 13	-11 ± 15	-2 ± 16
1.754	52 ± 1	-34 ± 3	41 ± 4	10 ± 5	-13 ± 6	36 ± 7	2 ± 7	-13 ± 8
1.782	53 ± 2	-40 ± 4	45 ± 5	31 ± 6	-18 ± 7	76 ± 8	-21 ± 8	12 ± 9
1.798	64 ± 2	-31 ± 4	59 ± 5	40 ± 5	-11 ± 6	99 ± 8	-16 ± 8	-13 ± 9
1.818	76 ± 3	-24 ± 6	92 ± 8	44 ± 9	5 ± 11	132 ± 13	-1 ± 13	27 ± 14
1.844	92 ± 5	2 ± 11	92 ± 14	40 ± 17	3 ± 19	127 ± 23	31 ± 24	-27 ± 29

C. From $K^- p \to \pi^- \Sigma^+$ (Polarization) × (Angular Distribution)

E_{CM}	$B_0 \times 10^{+3}$	$B_1 \times 10^{+3}$	$B_2 \times 10^{+3}$	$B_3 \times 10^{+3}$	$B_4 \times 10^{+3}$	$B_5 \times 10^{+3}$	$B_6 \times 10^{+3}$	$B_7 \times 10^{+3}$
1.732	0 ± 0	-50 ± 8	-42 ± 7	-17 ± 6	-2 ± 5	-4 ± 5	-2 ± 4	-4 ± 5
1.754	0 ± 0	-49 ± 6	-57 ± 5	-12 ± 4	3 ± 4	6 ± 4	-1 ± 3	-2 ± 3
1.782	0 ± 0	-47 ± 6	-65 ± 6	1 ± 4	-0 ± 4	8 ± 4	6 ± 3	1 ± 3
1.798	0 ± 0	-45 ± 7	-69 ± 6	-12 ± 5	-19 ± 5	3 ± 4	0 ± 4	3 ± 3
1.818	0 ± 0	-17 ± 9	-81 ± 8	-12 ± 7	-47 ± 7	-8 ± 6	-9 ± 6	-3 ± 5
1.844	0 ± 0	-23 ± 12	-7 ± 13	-45 ± 13	-8 ± 12	-0 ± 11	6 ± 10	6 ± 10

XBL 714-755

Table VIII. Summary of Fits

Fit	Parameterization D05	D15	F05	χ^2	DF	Causality Violation Wave	Speed
A	R(4)	R(4)	R(4)	258.9	238	P11	-3.1
B	R(4)	R(4)	R(3)	261.5	239	S01	-1.9
C	R(4)+P(4)	R(4)	R(3)	257.9	235	S11	-2.2
D	R(4)	R(4)+P(4)	R(3)	247.8	235	S11	-3.2

Table IX. Resonance Parameters

Resonance	Fit	Mass (GeV)	Amplitude $\sqrt{x_e x_r}$	Half-Width (GeV)	Relative Phase
D15	A	1.722	.086	.060	- .04
	B	1.727	.121	.039	-1.07
	C	1.766	.101	.040	- .30
	D	1.765	.068	.023	- .53
D05	A	1.825	.174	.028	4.05
	B	1.827	.174	.032	3.28
	C	1.830	.173	.029	3.71
	D	1.834	.170	.040	3.56
F05	A	1.836	.293	.048	3.99
	B	1.828	.288	.045	[3.14]
	C	1.826	.275	.048	[3.14]
	D	1.832	.284	.052	[3.14]

Figure Captions

Fig. 1. Distribution of fitted beam momenta for the Σ events. Numbers of events passing all cuts are shown per bin of .01 GeV/c.

Fig. 2. Comparison of non-Gaussian distributed fiducial quantities for Σ events. The cuts applied for these quantities are indicated.

Fig. 3. Decay vertex fiducial volume.

Fig. 4. Differential lifetime distributions--numbers of events weighted only for decay angle losses. The time intervals for $\Sigma^-(\Sigma^+)$ decays are .05 (.03) nsec.

Fig. 5. Decay angular distributions.

a. Azimuthal angle, ϕ, as described in Ref. 4.

b. Cosine of center of mass angle, $c = \cos \delta^*$, as defined in Ref. 4.

Fig. 6. Production angular distributions, showing sums of weighted events in the bin combinations. Widths of combinations are multiples of 0.1 in the production cosine, $\cos \theta = \hat{k}_K \cdot \hat{k}_\pi$.

a. $K^-p \to \pi^+\Sigma^-$

b. $K^-p \to \pi^-\Sigma^+$

Fig. 7. Polarizations for $K^-p \to \pi^-\Sigma^+$ in intervals of the production cosine, $\cos \theta$. The dashed curves show the functional representation calculated from the Legendre series expansions.

Fig. 8. Functional representation of the production angular distributions. The dashed curves are the Legendre series expansions in the production consine, $\cos \theta$; the shaded histograms give weighted numbers of events per bin of 0.1.

8. a. $K^-p \to \pi^+\Sigma^-$

b. $K^-p \to \pi^-\Sigma^+$

Fig. 9. Dalitz plots and invariant mass-squared distributions. Dashed curves in plots indicate kinematically imposed boundaries for each of the energies, E, included in the plot. Dashed curves over histograms indicate the average shape that would result from completely isotropic distribution of the final state momenta. The histograms are of weighted events per bin of 0.02 GeV^2. The quantities m_o^2, $m_\pm^2$ are defined in Ref. 4.

a. $K^-p \to \pi^+\Sigma^-\pi^o$

b. $K^-p \to \pi^-\Sigma^+\pi^o$. The Dalitz plots include events from both $\Sigma^+ \to \pi^o p$ and $\Sigma^+ \to \pi^+ n$; the invariant mass-squared distributions include only events from $\Sigma^+ \to \pi^+ n$.

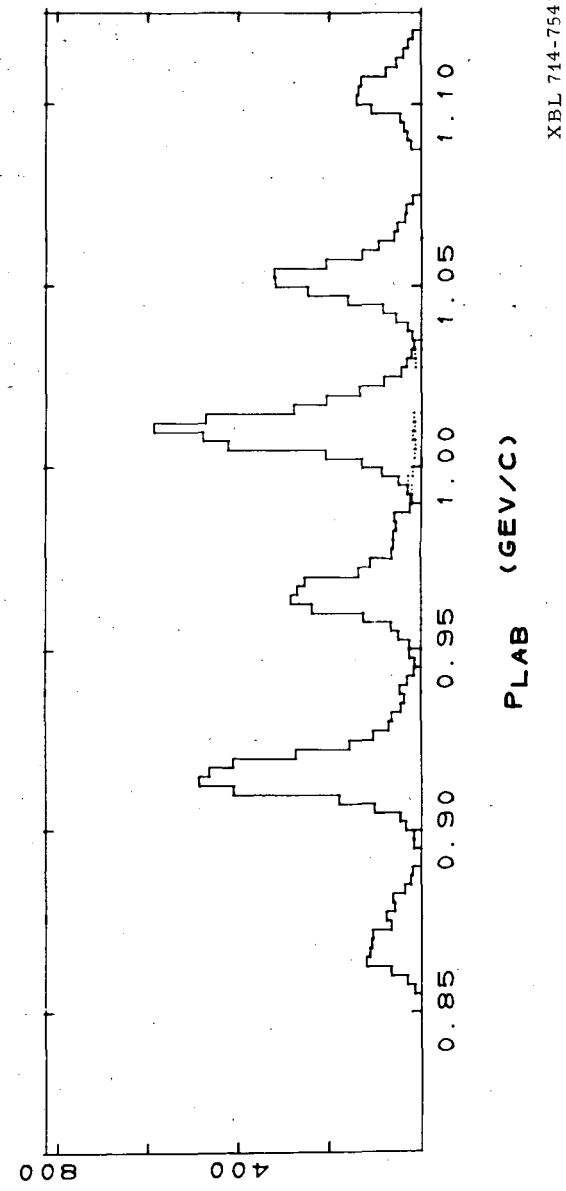

XBL 714-754

Fig. 1

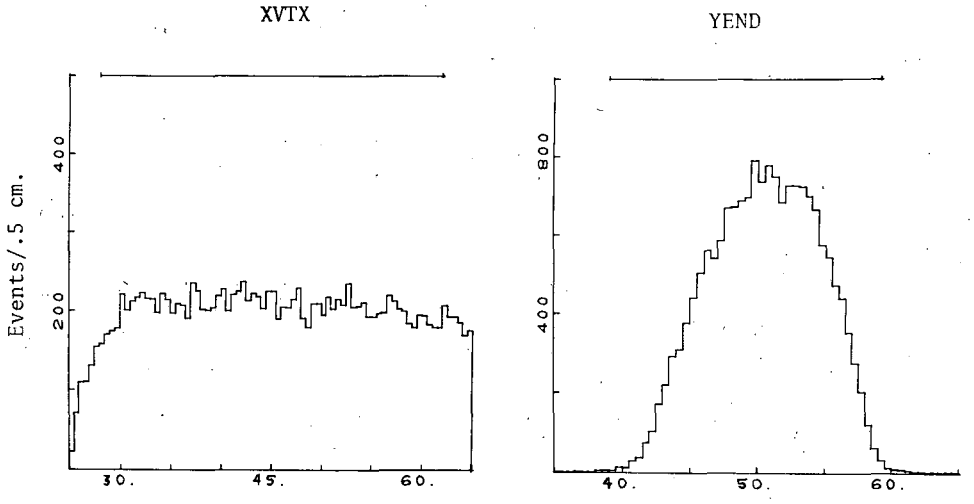

Fig. 2

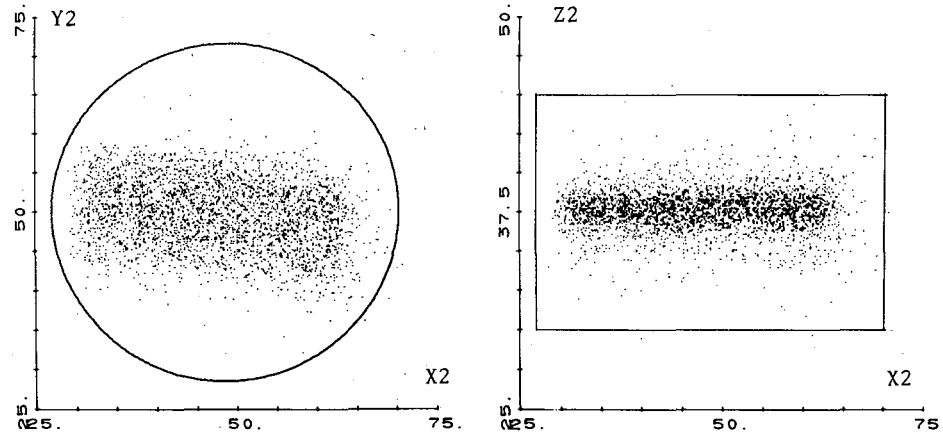

XBL 714-767

Fig. 3

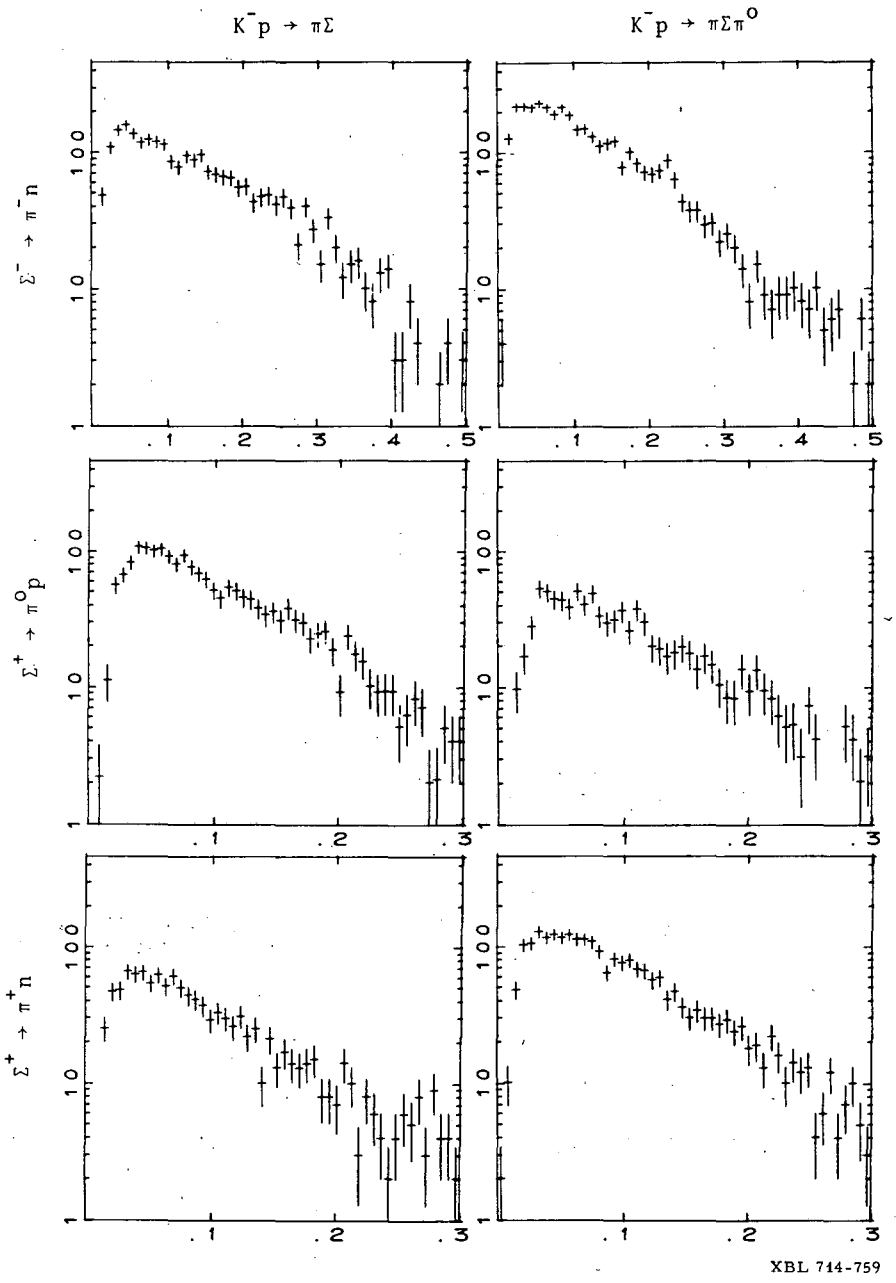

Fig. 4

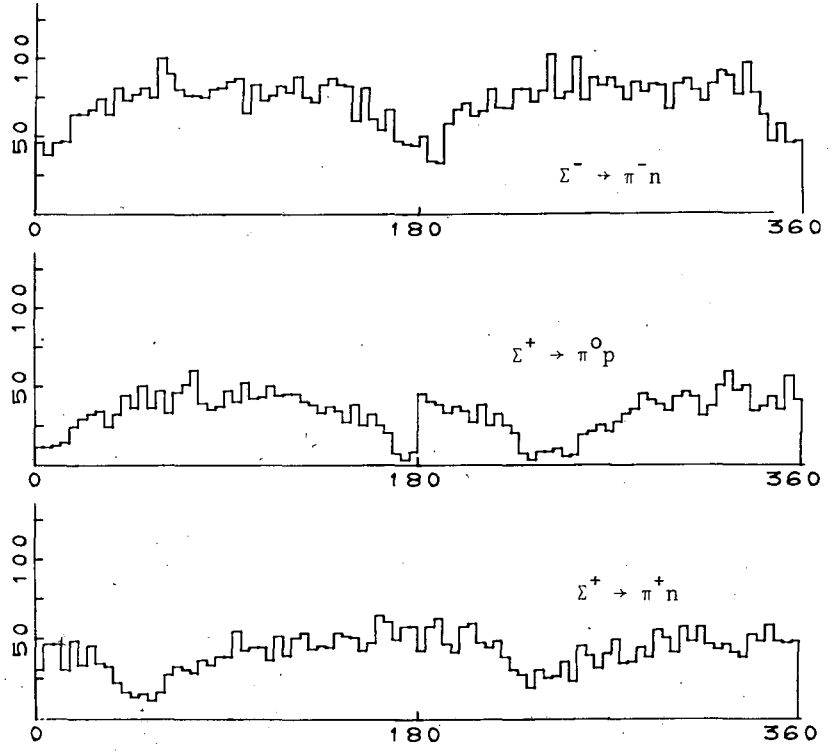

Fig. 5a

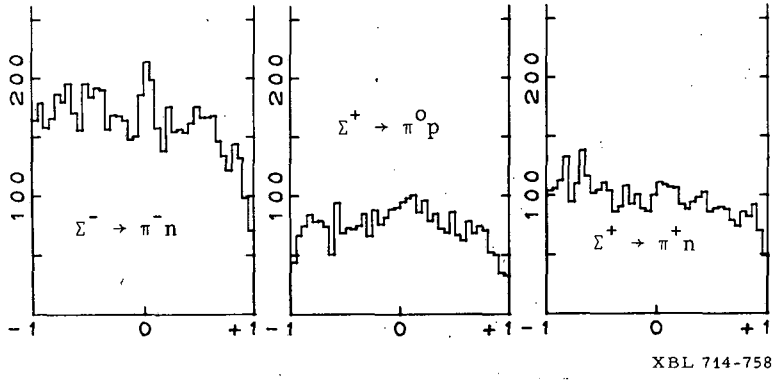

Fig. 5b

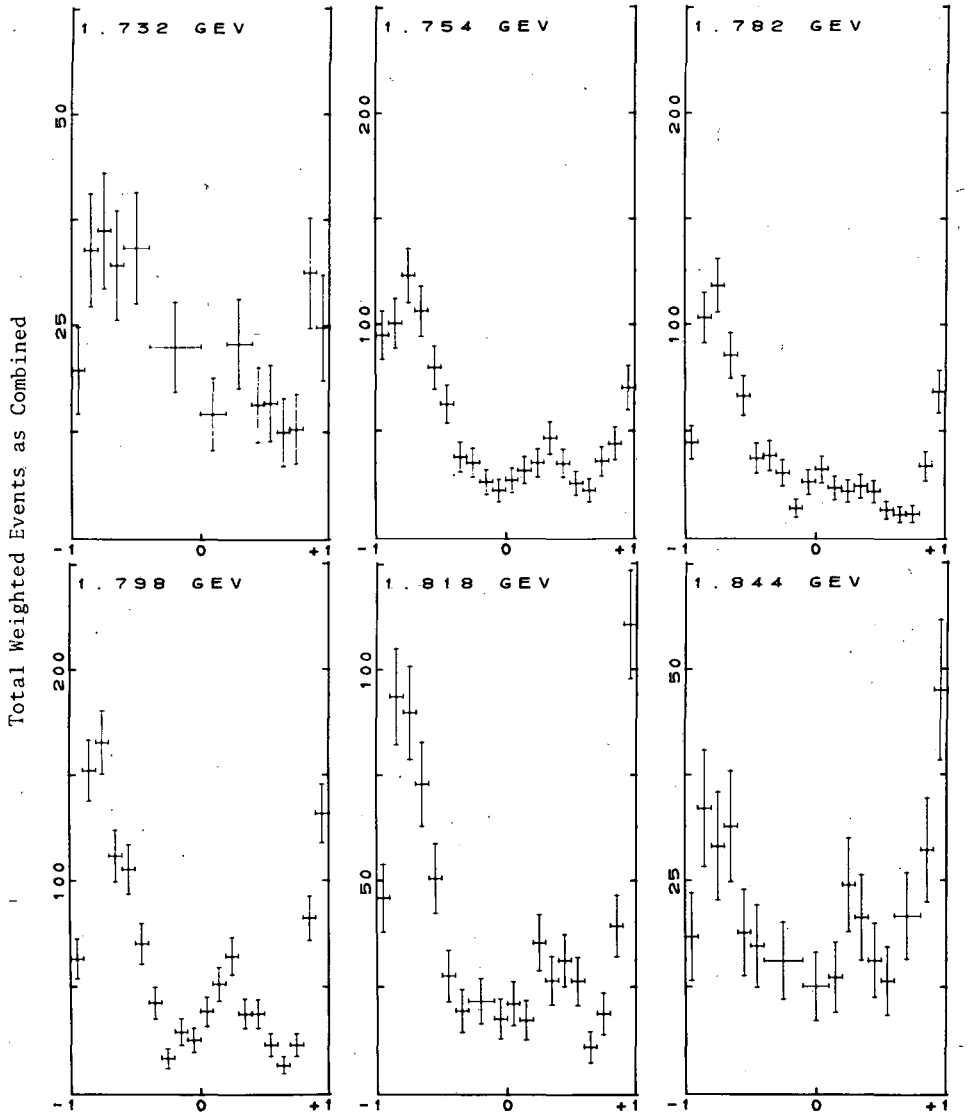

Fig. 6a

$K^- p \to \pi^+ \Sigma^-$

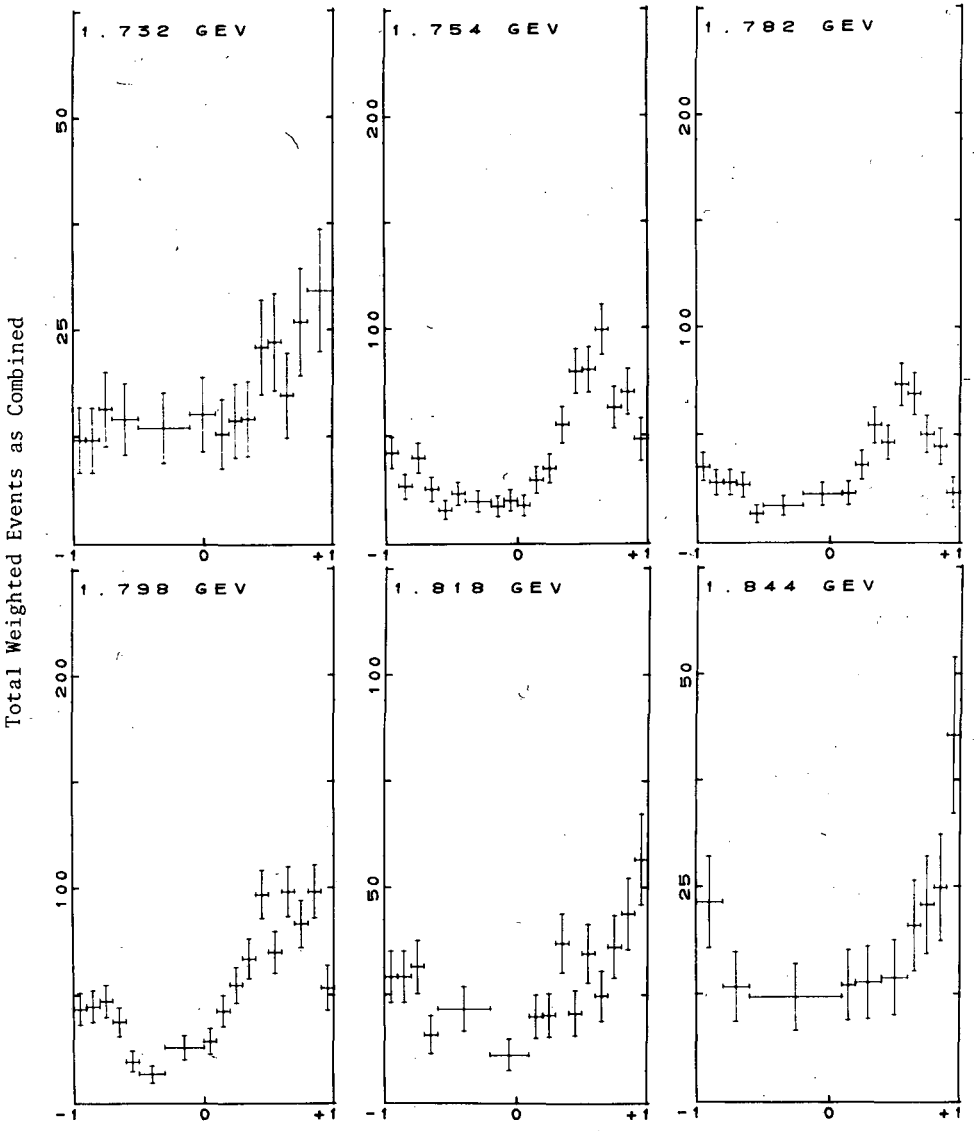

Fig. 6b

$K^- p \to \pi^- \Sigma^+$

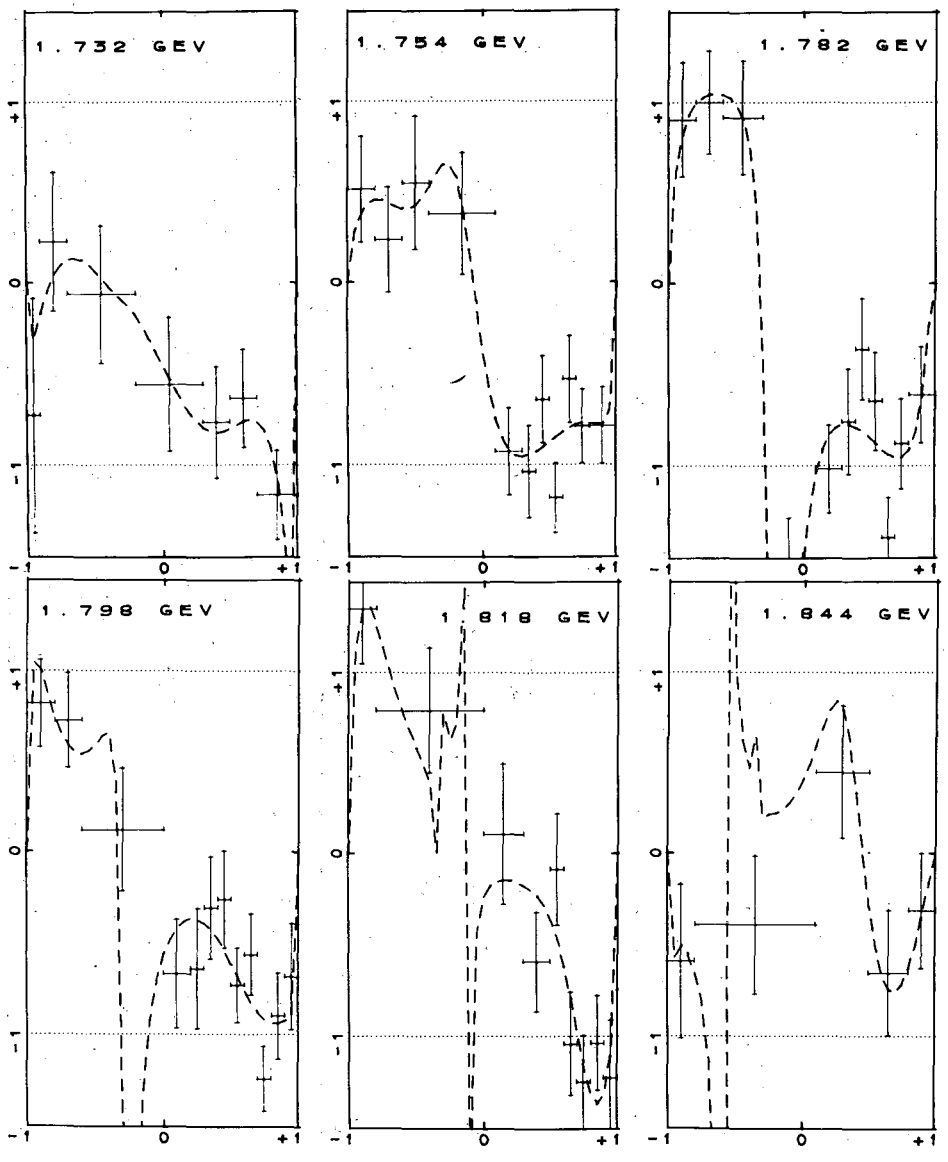

Fig. 7

$K^- p \to \pi^- \Sigma^+$

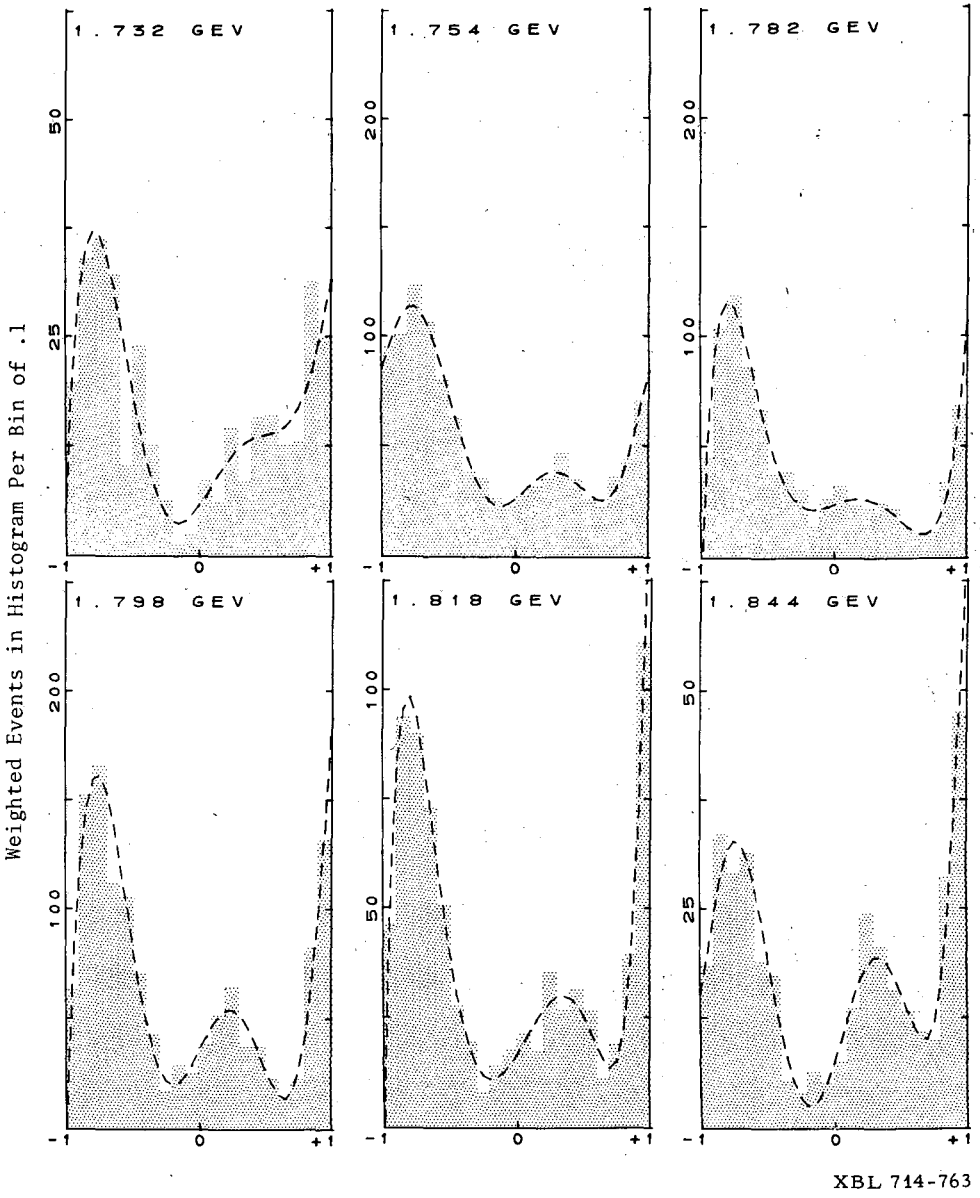

Fig. 8a

$K^- p \to \pi^+ \Sigma^-$

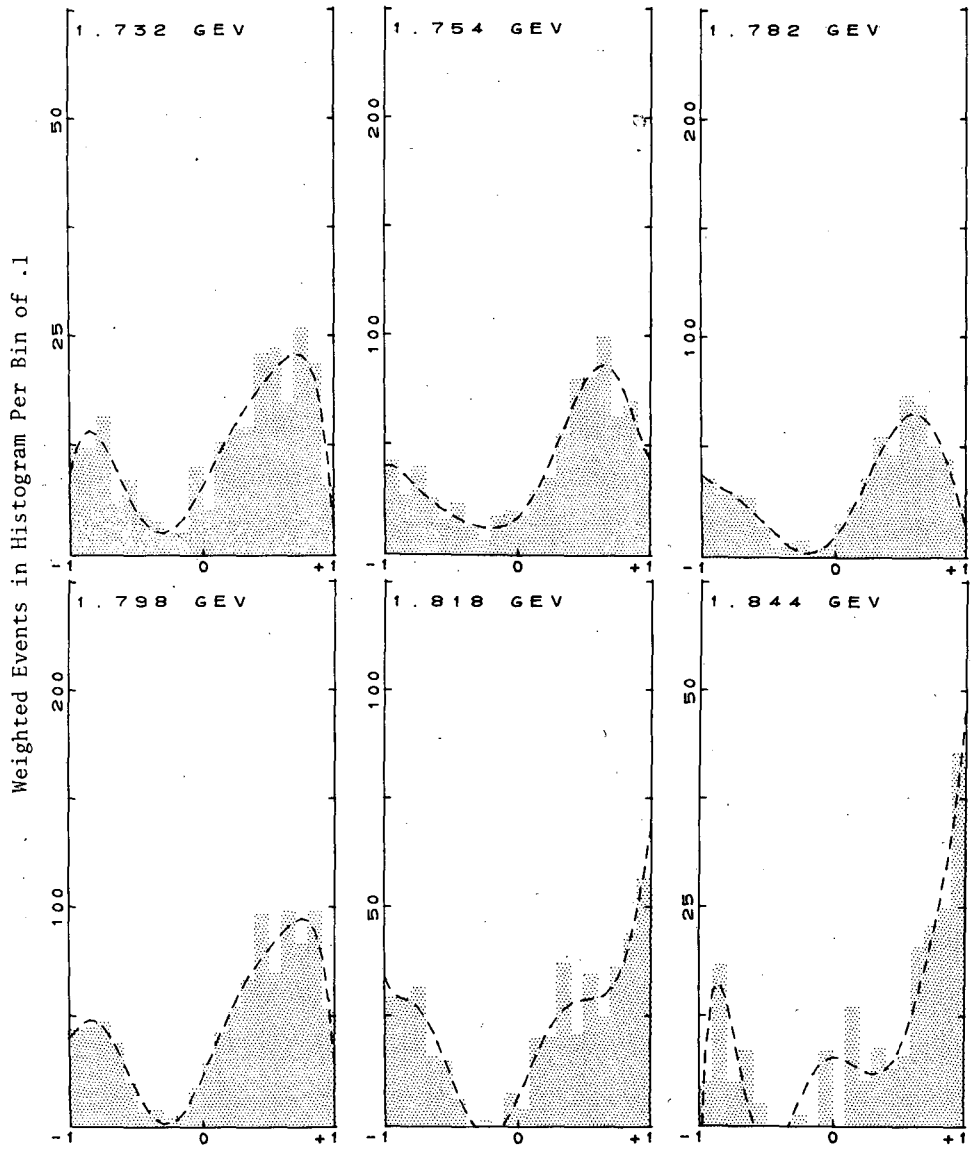

Fig. 8b

$K^- p \to \pi^- \Sigma^+$

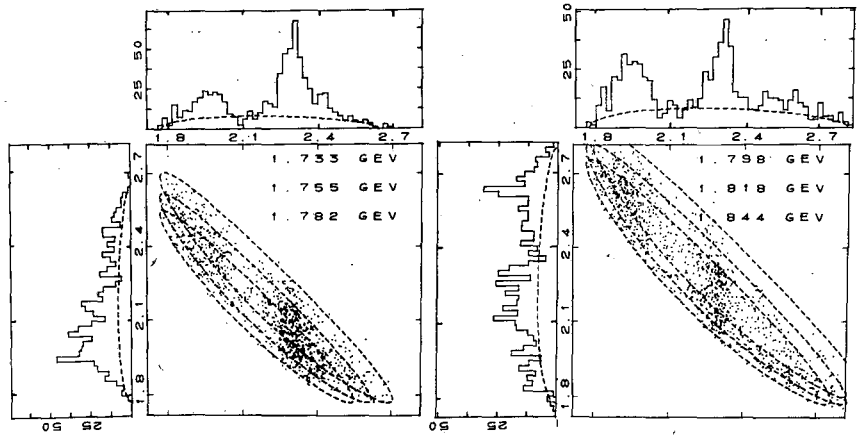

Fig. 9a. $K^- p \to \pi^+ \Sigma^- \pi^o$

Weighted events in histograms per bin of .02 GeV^2.

$m_\pm^2$ (GeV^2)

m_o^2 (GeV^2)

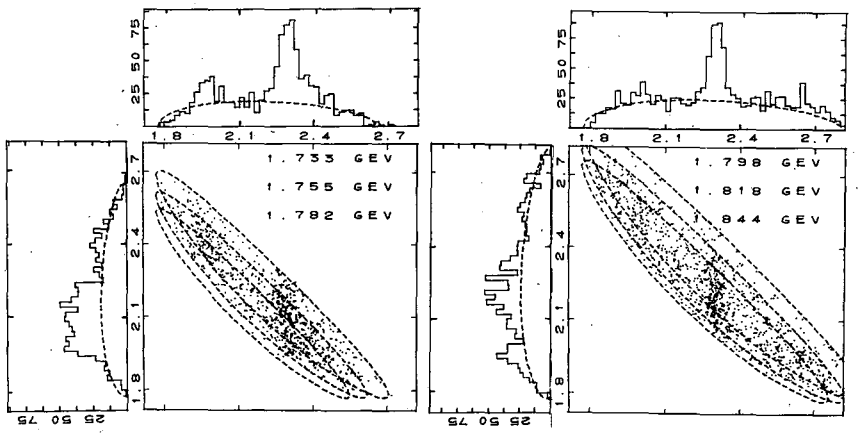

Fig. 9b. $K^- p \to \pi^- \Sigma^+ \pi^o$

TECHNICAL INFORMATION DIVISION
LAWRENCE BERKELEY LABORATORY
UNIVERSITY OF CALIFORNIA
BERKELEY, CALIFORNIA 94720